Element-specific magnetic moments in bcc $Fe_{81}Ni_{19}$/Co superlattices

I. L. Soroka,[1] M. Björck,[1] R. Bručas,[2] P. Korzhavyi,[3] and G. Andersson[1]
[1]*Department of Physics, Uppsala University, Box 530, SE-751 21 Uppsala, Sweden*
[2]*Department of Solid State Physics, Chalmers University of Technology, SE-412 96 Göteborg, Sweden*
[3]*Applied Materials Physics, Department of Material Science and Engineering, Royal Institute of Technology (KTH), SE-100 44 Stockholm, Sweden*
(Received 7 April 2005; revised manuscript received 5 August 2005; published 6 October 2005)

The magnetic moments in bcc $Fe_{81}Ni_{19}$/Co(001) superlattices with the individual layer thickness of 2–6 monolayers were studied by means of soft x-ray magnetic circular dichroism. It was found that the magnetic moment was enhanced in the $Fe_{81}Ni_{19}$ layer by about $0.35\mu_B$/atom as compared to the bulk value, while the Co moment remained unaffected by the presence of interfaces. The extension of the region with the high $Fe_{81}Ni_{19}$ moment in our samples was found to be at least 3 monolayers from the interfaces. Possible sources of the $Fe_{81}Ni_{19}$ moment enhancement were considered in *ab initio* calculations, and it was concluded that the enhanced moment may be explained by intermixing and formation of a B2-type short-range order at the interfaces.

DOI: 10.1103/PhysRevB.72.134409 PACS number(s): 75.25.+z, 75.70.−i

I. INTRODUCTION

Interface magnetism in magnetic multilayers and superlattices composed of 3*d* elements has been extensively studied both theoretically[1–3] and experimentally.[4–6] The reduced symmetry and lower coordination numbers lead to significant changes of magnetic moments at the interfaces as compared to the bulk values. One of the questions to be addressed in this context is the spatial distribution of magnetic moments. In multilayer films it depends on the changes in the electronic structure of the constituents [for example, due to the existence of metastable phases, such as body-centered-cubic (bcc) Co (Ref. 7) and bcc Ni (Ref. 8)], on the strain state[9] and on alloying or interdiffusion at the interfaces.[10]

In a number of studies on bcc Fe/Co multilayer films[2,11,12] it was shown that the Fe magnetic moment increases dramatically, by $0.4–0.8\mu_B$/atom, in the first layer and gradually decreases to its bulk value beyond a distance of 2–3 monolayers from the interface. At the same time, the Co moment is found to remain unaffected by the presence of the interfaces. However, in another study[13] an enhancement of the Co magnetic moment by about $0.4\mu_B$/atom at the interfaces has been deduced in Fe/Co superlattices, while for the Fe moment an oscillatory behavior has been claimed.

The magnetic moment of a tetragonally distorted bcc Ni layer in the Fe/Ni(001) superlattices is found to be enhanced to $0.85\mu_B$/atom and nearly constant for the Ni thickness in the range from 3 to 16 Å (Ref. 8). This enhancement is explained to be due to the reduced coordination number in the body-centered-tetragonal (bct) structure and to the interactions at the Fe/Ni interfaces. The Fe moment is also found to have a slightly higher value as compared to the bulk. The enhanced moment does not vary much until the multilayer undergoes a transition to a face-centered-tetragonal (fct) phase where the Fe moment is suppressed.

In our previous work we studied the influence of composition and interfaces on the magnetic properties of bcc $Fe_{81}Ni_{19}$/Co(001) superlattices.[14] The total magnetic moment was found to be enhanced in the interface region [with 3.5 monolayers (ML) thickness], as compared to the interior region. However, in that study the magnetic moment behavior of separate elements was not determined. In comparison to Fe/Co superlattices, the presence of Ni in the $Fe_{81}Ni_{19}$/Co superlattices decreases the magnitude of the anisotropy constant[15] and affects the value of the Fe magnetic moment[16] in bcc FeNi alloys.

As mentioned above, one possible reason for the magnetic moment changes at interfaces is the interface imperfections, such as roughness and interdiffusion,[17] that are always present in magnetic superlattices. These imperfections change the local environment for individual atoms and, hence, the local magnetic moments. The magnetic moments in Fe/V multilayers have recently been reproduced with reasonable accuracy by first-principle theory under the assumption of diffuse interfaces over two to three atomic layers on each side.[10]

Fe—Co alloys are known to form a bcc solid solution for temperatures higher than 700 °C. At lower temperature these alloys undergo a disorder-order transition towards a B2 structure. For example, the B2 phase is stable for Fe concentrations in the range from 18 to 80 at. % at 250 °C,[18] which is the optimal substrate temperature for the Fe/Co superlattice growth.[12] Therefore, the existence of a short-range ordered B2-type phase[19] is to be considered when discussing the interface formation in bcc Fe/Co superlattices.

In the present investigation we perform an element-specific analysis of the magnetic moments in bcc $Fe_{81}Ni_{19}$/Co(001) superlattices by means of x-ray magnetic circular dichroism (XMCD) magnetometry at the L_2 and L_3 absorption edges. Though XMCD has proved to be a powerful tool to probe the element specific and layer resolved[20] magnetic properties, it is a surface sensitive technique. Such details as surface oxidation or the presence of an interface between the film and the capping layer may give considerable contributions to the dichroic signal. One way to minimize the contribution from the capping layer is to use an

additional spacer layer between the capping and the studied magnetic layer. Therefore, two sets of superlattices where the top layer before the capping layer was either Co or $Fe_{81}Ni_{19}$, were specially grown. The obtained experimental results are analyzed with the help of *ab initio* calculations.

II. EXPERIMENTAL PROCEDURE

A. Growth and structural characterization

Body-centered-cubic $Fe_{81}Ni_{19}$/Co(001) superlattices were grown on single crystal MgO(001) substrates by dc magnetron sputtering from separate $Fe_{81}Ni_{19}$ (99.99% purity; the target composition is given in weight percent) and Co (99.95%) targets arranged in a cluster geometry. The $Fe_{81}Ni_{19}$ target was presputtered for about 10 minutes in order to reach a steady state when the surface composition of the alloy target adjusts itself to balance the difference in the sputtering yields of the constituents and the composition of the sputtered flux starts to resemble the composition of the target.[21] The base pressure in the chamber was lower than 3×10^{-9} torr and the operating pressure of Ar gas was kept at 1.5 mtorr. The resulting deposition rates were 0.37 Å/s and 0.64 Å/s for $Fe_{81}Ni_{19}$ and Co, respectively. The deposition rates were obtained *in situ* by a calibrated quartz crystal microbalance. The optimal substrate temperature during the growth of 270 °C was determined in our previous study[14] and used here.

To prevent oxidation, the as-grown films were capped with a 10 Å thick Al_2O_3 layer. In order to minimize the influence of the capping layer on XMCD measurements, two sets of superlattices were prepared. The first set of specimens was used for determination of the Fe and Ni magnetic moments, and therefore the thickness of the $Fe_{81}Ni_{19}$ layer was varied from 2 to 6 ML, whereas the Co layer thickness was kept constant and equal to 6 ML. The final layer beneath the cap was a 6 ML thick layer of Co. In the other set of specimens we varied the Co layer thickness from 2 to 6 ML, while keeping the $Fe_{81}Ni_{19}$ layer thickness constant at 6 ML, and 6 ML of $Fe_{81}Ni_{19}$ was the final layer. The constant thickness equal to 6 ML of the $Fe_{81}Ni_{19}$ (Co) layer was chosen for the following reasons: first, this layer should be thin enough to enable measurement of the electron yield from at least one bilayer, considering the effective electron escape depth of the order of 20 Å.[22] Second, it should be rather thick to eliminate the influence on the net magnetic moment from the atoms of the same kind in the next layer.[12]

The total number of repetitions was 25 for all samples. To obtain good lattice matching with the MgO (001) substrate, $Fe_{81}Ni_{19}$ was the initial layer in all the samples studied here. To estimate the Co thickness we used the lattice parameter for bcc Co, equal to 2.82 Å.[23]

The structural quality, the out-of-plane lattice parameter and the thickness of a bilayer in the superlattices were determined by x-ray diffraction (XRD) and x-ray reflectivity (XRR) measurements using a Siemens D5000 diffractometer with Cu K_α radiation, $\lambda=1.54$ Å. In Fig. 1 we present XRR patterns obtained from the set of $Fe_{81}Ni_{19}$/Co superlattices where the $Fe_{81}Ni_{19}$ layer thickness is varied. As seen in the figure all the samples exhibit superlattice peaks, indicating a compositional modulation along the film growth direction. The simulation of the reflectivity data (the dashed lines) using grazing incidence x-ray analysis (GIXA) (Ref. 24) yielded layer thickness variation, i.e., roughness or interdiffusion, in the range from 1.5 ML (in the 6/6 sample) to 2 ML (in the 2/6 sample). Despite the fact that in the reflectivity pattern the long wave modulation due to the capping Al_2O_3 layer was not included in the simulation, the intensities of the superlattice peaks in the measured and simulated curves fit well to each other.

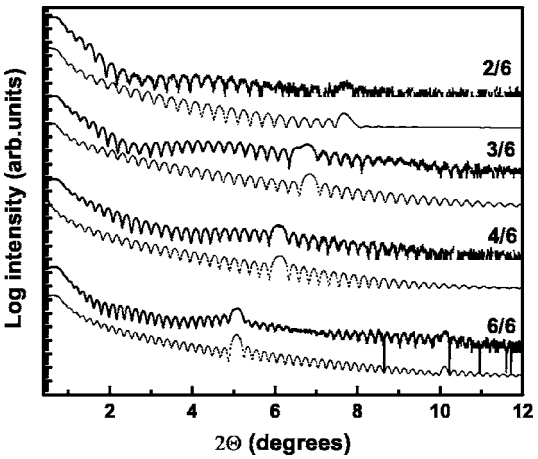

FIG. 1. Low angle reflectograms (solid lines) for the series of $Fe_{81}Ni_{19}$/Co superlattices along with the simulated patterns (dotted lines). The labels on the graph correspond to the amount of $Fe_{81}Ni_{19}$/Co expressed in monolayers. Note that the Al_2O_3 capping layer, 10 Å thick, is not included in the simulation.

XRD measurements were carried out in Bragg-Brentano geometry in the angular region $2\theta=20°-100°$ for all the superlattices. A representative XRD pattern for the 6/6 superlattice is shown in Fig. 2. Only one Bragg peak at $2\theta\approx65°$, which corresponds to the (002) reflection from the bcc $Fe_{81}Ni_{19}$/Co lattice, was found. No other diffraction peaks except for the substrate were observed, indicating the absence of additional phases and crystal orientations. The main peak was surrounded by satellites which appeared be-

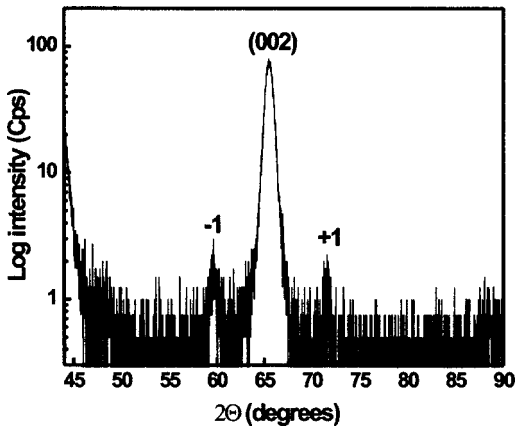

FIG. 2. High angle x-ray diffraction pattern for the $Fe_{81}Ni_{19}$(6 ML)/Co(6 ML) superlattice. The rise of the background at the low angle side is due to the MgO(002) peak.

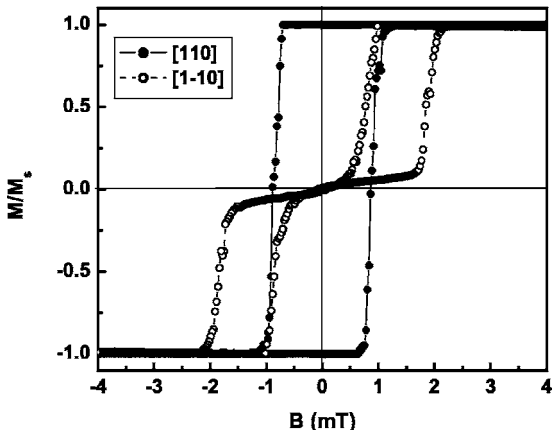

FIG. 3. Room temperature magnetization hysteresis loops of the $[Fe_{81}Ni_{19}(6\ ML)/Co(6\ ML)]_{25}$ superlattice, normalized to a saturation magnetization, M_s.

cause of the chemical periodicity of the structure. The intensities of these peaks were rather low even for 6/6 sample, due to both the small total thickness (425 Å) of the film and the similar x-ray scattering atomic form factors for Fe and Co. The satellites became less pronounced for thinner films, and no satellite peaks were observed for the superlattices with the thinnest $Fe_{81}Ni_{19}$(Co) layers. The out-of-plane crystal coherence length was derived from the full width at half-maximum (FWHM) of the (002) peak, and its lower limit was found to be about 100 Å for the 6/6 sample. For the other superlattices the crystal coherence length was varying in the range from 90 Å to 115 Å. Since the crystal coherence length is much larger than the bilayer thickness, the films can be considered to have a superlattice structure.

A more detailed structural study of the $Fe_{81}Ni_{19}$/Co superlattices was performed in our previous work,[14] where the average in-plane lattice constants and the individual lattice parameters of the constituents ($c_{Fe_{81}Ni_{19}}=2.89$ Å, $c_{Co}=2.82$ Å) were determined. In addition, the maximum tetragonal distortions expressed in c/a ratio were found to be 1.02 for $Fe_{81}Ni_{19}$ and 0.99 for Co.

B. Magnetic characterization

The easy direction of magnetization in the superlattices was determined using a magneto-optical Kerr effect (MOKE) setup in a longitudinal geometry. Hysteresis loops were recorded for various orientations of the applied magnetic field with respect to the in-plane crystallographic directions.

In Fig. 3 we show typical magnetization loops measured along the two orthogonal in-plane [110] and $[1\bar{1}0]$ directions. As seen from the figure, if the field is applied in the easy [110] direction the hysteresis loop has an oblique rectangular shape with 100% remanence. When the field is applied along the $[1\bar{1}0]$ direction, the magnetization reversal occurs in two steps and at $B=0$ the moments spontaneously line up parallel to the [110] direction. The saturation field in the hard [100] direction (the hysteresis loop is not shown here) is about 40 mT. For further details see Ref. 25

The presence of the in-plane uniaxial anisotropy in the films investigated here needs to be considered in the XMCD measurements, since in order to obtain maximum signal all electron spins should be aligned parallel or antiparallel to the photon propagation direction. Therefore, prior to each XMCD measurement the samples were magnetized in the [110] direction using a pulsed electromagnet, and the measurements were carried out in the remanent state.

The XMCD measurements at the L_2 and L_3 absorption edges of Fe, Co, and Ni were carried out at beamline D1011, at the Swedish synchrotron radiation facility MAX-lab, using monochromatized radiation with a degree of circular polarization $P_c=0.85$.[26] The angle of incidence in the present measurements was 45° relative to the sample surface.

The XMCD signal is the difference in absorption between the right and the left circularly polarized x rays near the atomic absorption edge. It was measured by reversing the magnetization direction of the sample for a fixed photon helicity, which is equivalent to changing the polarization. The absorption spectra were recorded in remanence through the total electron yield. The energy intervals of 670–770 eV, 740–840 eV, and 820–920 eV were used for Fe, Co, and Ni, respectively. Each spectrum was acquired 3 times in order to verify reproducibility. In order to reliably quantify the magnetic moments, two reference samples were measured as well. They consisted of a 300 Å thick $Fe_{81}Ni_{19}$ or Co single layer, capped with 10 Å of Al_2O_3. All the measurements were performed at room temperature.

The x-ray absorption spectra for the two opposite magnetization directions were converted into dichroism spectra using a standard procedure. First, a linear background was subtracted to make the pre-edge and the post-edge regions coincide. Then both spectra were normalized to a constant edge jump with the normalization constant determined from the data far above the Co L_2 edge, since the size of the edge jump far from the absorption edge is independent of the local atomic environment and is proportional to the number of atoms.[27] The difference spectra were determined from these normalized individual absorption spectra. In Fig. 4 we present the normalized absorption spectra (upper curves) and the difference spectra (lower curves) for Fe and Co.

The absorption and difference spectra for Ni are not presented here, since the yield from Ni was too low to quantify its dichroic signal. However, in our study we consider the Ni magnetic moment to be constant and equal to $m_{Ni}=0.93\mu_B$/atom. This value corresponds to the Ni moment in a bulk FeNi alloy which contains 80% Fe.[16] The ratio of the constituents in the FeNi film is expected to be conserved[21] and to correspond to the sputtering target composition.[28]

Analysis of the spectra was done using magneto-optical sum rules for the orbital[29] and spin[30] magnetic moments, which relate the integrated signal to the ground state properties. However, the uncertainty in the determination of those moments is rather large.[31] This is due to the fact that the number of valence holes is not exactly known and, also, the separation of the areas under the L_2 and L_3 peaks is not well defined. In our case the number of valence holes per unit area was obtained by measuring pure $Fe_{81}Ni_{19}$ and Co films (reference samples) and assuming that their magnetic moments

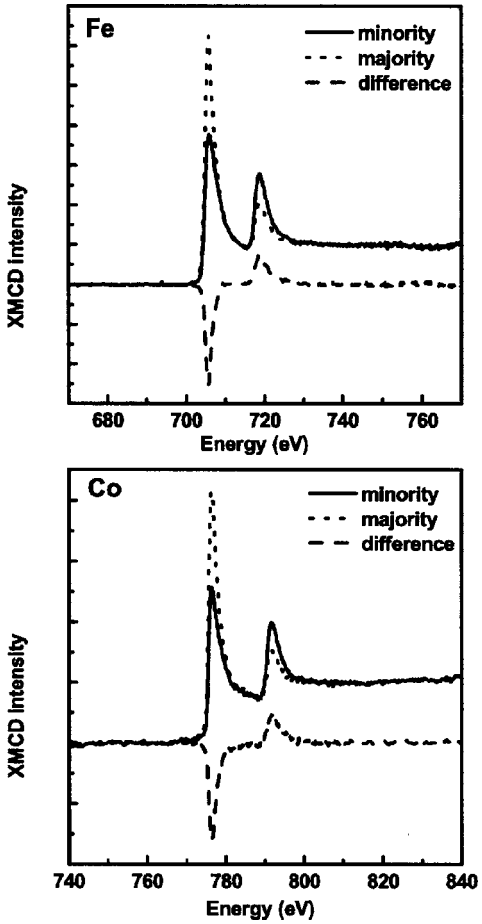

FIG. 4. Normalized x-ray absorption of Fe (a) and Co (b) in the $[Fe_{81}Ni_{19}(6\ ML)/Co(6\ ML)]_{25}$ superlattice taken with the projection of the incident photon spins parallel (solid line) and antiparallel (dotted line) to the spin of the 3*d* majority electrons. The lower parts of the figures (dashed line) show the XMCD signal in the difference spectra.

are equal to the bulk values taken from the literature. In Ref. 16 the magnetic moment of Fe, equal to $m_{Fe}=2.41\mu_B$/atom in $Fe_{81}Ni_{19}$ alloy, was determined by neutron diffraction measurements; for Co, a range of values between $1.53\mu_B$/atom and $1.75\mu_B$/atom have been reported[2,23,32–34] and $m_{Co}=1.72\mu_B$/atom[2,32] is used here. To suppress the uncertainty in the separation of the area under L_2 and L_3 peaks, the spectra should be treated in the same way.[12] The saturation effect was monitored and found to be negligible. Due to the lack of information about separate spin and orbit magnetic moments for Fe in $Fe_{81}Ni_{19}$ alloys, we consider just the total magnetic moment changes in the present investigation.

III. RESULTS AND DISCUSSION

In Fig. 5 we present the measured total magnetic moment for Fe and Co as a function of the individual layer thickness. As the figure shows, the magnetic moments of Co are rather similar for the interface and bulk environments, reflecting the fact that the Co spin-up band is almost completely filled. The average value of the magnetic moment for Co layers,

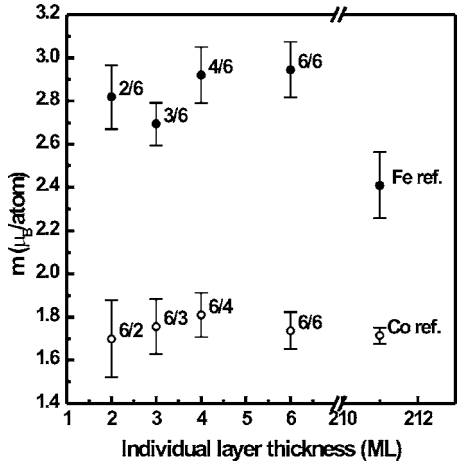

FIG. 5. Magnetic moments as determined by experiment for Fe (filled circles) and Co (open circles) versus the individual layer thickness. The error bars correspond to the relative errors obtained from the analysis. The labels on the graph correspond to the $Fe_{81}Ni_{19}$/Co layer thicknesses expressed in ML.

$1.75\pm0.14\mu_B$/atom, is close to the bulk value for bcc Co.

The Fe magnetic moment in thin layers is considerably enhanced relative to the bulk value for Fe (marked as "Fe ref." in Fig. 5) in a random $Fe_{81}Ni_{19}$ alloy. These results are in line with the experimental[7,12] and theoretical[2,3] studies of the Fe/Co superlattices. Besides, the Fe moments in $Fe_{81}Ni_{19}$/Co superlattices are affected by the Ni atoms and are found to be smaller than the iron moments, of about $3\mu_B$/atom, in iron-cobalt superlattices and alloys.[4]

As seen in Fig. 5, the Fe moment does not show the tendency to decrease with increasing $Fe_{81}Ni_{19}$ layer thickness. On the contrary, it shows a slight upturn. However, this increase of the Fe magnetic moment as a function of layer thickness is within the experimental error bars, and, therefore, the Fe moment may be considered to be nearly constant in the layers in the studied thickness range. It indicates that Fe atoms, even in the 6 ML thick layer, are influenced by the presence of interfaces, i.e., the interface region in which the moments are enhanced may be as thick as 3 ML. This is in agreement with our previous investigations,[14] where the extension of the interface region with enhanced moment in the $Fe_{81}Ni_{19}$/Co multilayers was concluded to be about 3.5 ML. Yet, in that study we did not determine at which side the enhancement occurred. Since the present measurement shows that the enhancement occurs on the Fe side, even a 7 ML thick $Fe_{81}Ni_{19}$ layer can entirely belong to the interface-affected region. Using the data presented in Fig. 5, we estimate the average magnetic moment of Fe to be $\langle m_{Fe}\rangle = 2.84\pm0.16\mu_B$/atom. Thus, the enhancement of the Fe moment is about $0.43\mu_B$/atom. Taking into consideration the amount of Fe in the $Fe_{81}Ni_{19}$ layers, we can extract the average magnetic moment ($2.45\mu_B$/atom) and its enhancement as being of the order of $0.35\mu_B$/atom in the $Fe_{81}Ni_{19}$ layer and, hence, in the $Fe_{81}Ni_{19}$/Co superlattices. Note that this value is rather close to the value of $0.3\mu_B$/atom extracted from the magnetic analysis in the previous study.[14] Even though the assumption of a constant Ni moment may be questioned, it is clear that even a ±50% change in the Ni

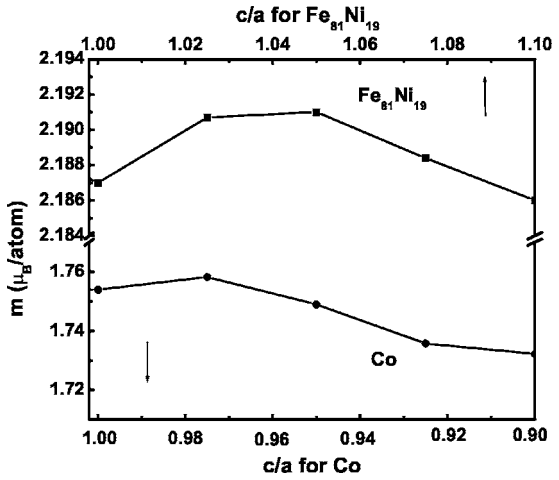

FIG. 6. Calculated spin moments in bulk body-centered-tetragonal $Fe_{81}Ni_{19}$ and Co as a function of the c/a ratio.

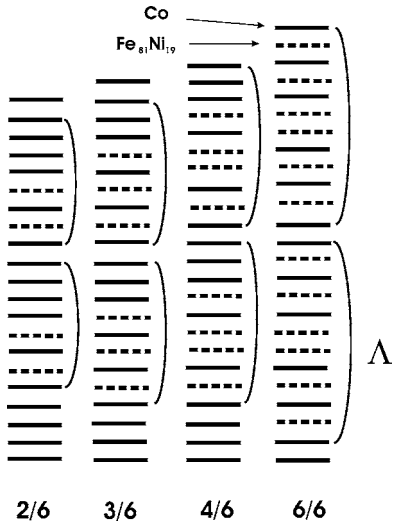

FIG. 7. A schematic illustration of the optimized layered structures, considered in the calculations. Λ is a bilayer thickness.

moment would contribute only $\pm 0.1\mu_B$/atom to the average moment of the $Fe_{81}Ni_{19}$ layer, which is within the experimental uncertainty.

Possible sources of the Fe moment enhancement in the $Fe_{81}Ni_{19}$/Co superlattices, such as tetragonal distortions and change in the local environment of Fe atoms due to the interface roughness or interdiffusion, have been analyzed, by comparing the experimentally measured magnetic moments with the values obtained using *ab initio* calculations discussed below.

Magnetic moment enhancement in 3*d* metal superlattices may occur due to tetragonal distortions[9] that develop in the individual layers during the superlattice formation. It was determined by structural analysis of the $Fe_{81}Ni_{19}$/Co superlattices that the $Fe_{81}Ni_{19}$ layers are slightly expanded and that the Co layers are compressed along the c axis.[14] The measured maximum c/a ratios are 1.02 and 0.99 for $Fe_{81}Ni_{19}$ and Co, respectively. In Fig. 6 we display the *ab initio* calculated spin moments as functions of c/a ratio. The calculations have been performed using the Korringa-Kohn-Rostoker method in the coherent potential approximation (KKR-CPA) (Ref. 35) for the bulk $Fe_{81}Ni_{19}$ and Co. As seen from the figure, tetragonal distortions in the studied superlattices give rise to a very small spin moment enhancement, about $0.005\mu_B$/atom for $Fe_{81}Ni_{19}$ and $0.01\mu_B$/atom for Co. Although, the orbital moment is more sensitive to the tetragonal distortions than the spin moment, its contribution to the total moment enhancement will hardly exceed the uncertainty of our experiment $0.1\mu_B$/atom, since the orbital moment in 3*d* metals is at least one order of magnitude smaller than the spin moment.[36]

Another source of magnetic moment enhancement can be the change in local environment of the Fe atoms, introduced by the interface imperfections such as alloying or interdiffusion. As has been shown previously[2,3] in superlattices with atomically sharp interfaces, the Fe magnetic moment is enhanced in the first monolayer near the interface, and then it rapidly decreases with distance to the bulk value. In the presence of interdiffusion and alloy formation at the interfaces, the magnetic moments are expected to follow the Slater-Pauling curve, as a function of the alloy concentration. In addition, the high values of magnetic moments measured in the current study may indicate the presence of a short-range order in the superlattices.

Indeed, the sample preparation conditions allowed for a limited intermixing of the constituents during the superlattice growth. The substrate temperature of 270 °C was below the temperature of B2 ordering in the Fe—Co binary system, so that some degree of a short-range order between the Fe and Co atoms might have developed as a result of intermixing at the interfaces. Unfortunately, due to the similarity in scattering properties of Fe, Co, and Ni, it is difficult to extract detailed information on the concentration profile from the results of x-ray diffraction measurements. Therefore, we made an attempt to simulate the effect of alloy formation at the interfaces using *ab initio* KKR-CPA calculations for $Fe_{81}Ni_{19}$/Co superlattices. First of all in these calculations, we compared the total energies of the ordered and disordered $Co_{50}Fe_{40}Ni_{10}$ alloy phases and found that the ordered phase possesses lower energy and also higher magnetic moment than the disordered one. Thereafter, we adopted a repeated slab geometry and took the experimental[14] values for the in-plane lattice parameters and for the interlayer distances. Several structures with different degrees of intermixing have been considered, aiming at simultaneously maximizing the Fe magnetic moments and minimizing the total energy, while preserving the superlattice periodicity. All the considered structures may be derived from the structures with ideally sharp interfaces (no intermixing) by a series of subsequent exchanges of the neighboring (001) $Fe_{81}Ni_{19}$ and Co layers. This optimization procedure results in the structures shown in Fig. 7. It is noteworthy that, in spite of the severe layer intermixing and well-developed B2-type short-range order, all these structures preserve the initial superlattice reflection, while the B2 superstructure peak is suppressed due to the presence of antiphase boundaries in the structures.[37] In Fig. 8 we compare the calculated average spin moments in the $Fe_{81}Ni_{19}$ layers for the optimized structures with the magnetic moments derived from XMCD experiments. Keeping

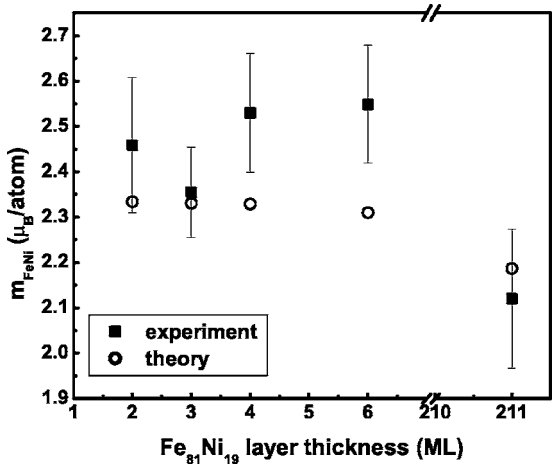

FIG. 8. Experimental (filled squares) and theoretical (open circles) values of the magnetic moments in the $Fe_{81}Ni_{19}$ layers versus $Fe_{81}Ni_{19}$ layer thickness, for constant Co layer thickness equal to 6 ML. In the theoretical calculation only the spin magnetic moment is considered.

in mind that, in order to fully enable the comparison, one should add an orbital moment value of about $0.1\mu_B$/atom[38] to the calculated spin moment values, the agreement between theory and experiment is very reasonable. Also, the present calculations have confirmed the experimental observation that the spin moment for Co atoms is insensitive to their local environment. The proposed model structures are the simplest structures that meet the following main criteria: they have magnetic moments of the constituents which are close to the experimental values, and, at the same time, they preserve superlattice periodicity. Further optimization of the structure in order to achieve a more realistic concentration profile (with partial intermixing etc.) is impractical at the present stage. More detailed experimental information on the concentration profile is highly desirable for further refinement of the present theoretical model. This information may be obtained, for instance, from neutron scattering experiments.

IV. CONCLUSIONS

The element-specific magnetic moments in bcc (001) $Fe_{81}Ni_{19}$/Co superlattices have been studied using x-ray circular dichroic magnetometry at the L_2 and L_3 absorption edges. The measurements have shown that the magnetic moments of the $Fe_{81}Ni_{19}$ layers are enhanced by $0.35\mu_B$/atom relative to the bulk value and are equal to $2.45\mu_B$/atom, on average. The extension of the region with the enhanced $Fe_{81}Ni_{19}$ moment in our samples is found to be at least 3 ML from the interface. Meanwhile, the Co moment remains unaffected and equal to $1.75\mu_B$/atom. This value is rather close to the bulk magnetic moment of Co, $1.72\mu_B$/atom. We have analyzed possible sources of enhancement of the $Fe_{81}Ni_{19}$ moment using *ab initio* calculations and concluded that it can mainly be ascribed to intermixing and formation of a B2-type short-range order at the interfaces.

ACKNOWLEDGMENTS

The financial support from the Swedish Foundation for Strategic Research (SSF) is acknowledged. One of the authors (I. L. S.) would like to acknowledge the discussions of the results with Björgvin Hjörvarsson. The authors would also like to thank Alexei Preobrajenski for practical assistance at MAX-lab.

[1] H. Hasegawa, J. Phys.: Condens. Matter **4**, 169 (1992).
[2] A. M. N. Niklasson, B. Johansson, and H. L. Skriver, Phys. Rev. B **59**, 6373 (1999).
[3] O. Eriksson, L. Bergqvist, E. Holmström, A. Bergman, O. LeBacq, S. Frota-Pessoa, B. Hjörvarsson, and L. Nordström, J. Phys.: Condens. Matter **15**, S599 (2003).
[4] S. Pizzini, A. Fontaine, E. Dartyge, C. Giorgetti, F. Baudelet, J. P. Kappler, P. Boher, and F. Giron, Phys. Rev. B **50**, 3779 (1994).
[5] F. Wilhelm, P. Poulopoulos, G. Ceballos, H. Wende, K. Baberschke, P. Srivastava, D. Benea, H. Ebert, M. Angelakeris, N. K. Flevaris, D. Niarchos, A. Rogalev, and N. B. Brookes, Phys. Rev. Lett. **85**, 413 (2000).
[6] C. L. Canedy, X. W. Li, and G. Xiao, Phys. Rev. B **62**, 508 (2000).
[7] J. Dekoster, E. Jedryka, M. Wójcik, and G. Langouche, J. Magn. Magn. Mater. **126**, 12 (1993).
[8] Tao Lin, M. M. Schwickert, M. A. Tomaz, H. Chen, and G. R. Harp, Phys. Rev. B **59**, 13911 (1999).
[9] T. Burkert, L. Nordström, O. Eriksson, and O. Heinonen, Phys. Rev. Lett. **93**, 027203 (2004).
[10] E. Holmström, L. Nordström, L. Bergqvist, B. Skubic, B. Hjörvarsson, I. A. Abrikosov, P. Svedlindh, and O. Eriksson, Proc. Natl. Acad. Sci. U.S.A. **101**, 4742 (2004).
[11] B. Kalska, P. Blomqvist, L. Häggström, and R. Wäppling, J. Phys.: Condens. Matter **13**, 2963 (2001).
[12] M. Björck, G. Andersson, B. Lindgren, R. Wäppling, V. Stanciu, and P. Nordblad, J. Magn. Magn. Mater. **284**, 273 (2004).
[13] P. Blomqvist, R. Wäppling, A. Broddefalk, P. Nordblad, S. G. E. te Velthuis, and G. P. Felcher, J. Magn. Magn. Mater. **248**, 75 (2002).
[14] I. L. Soroka, R. Bručas, V. Stanciu, P. Nordblad, and B. Hjörvarsson, J. Magn. Magn. Mater. **277**, 228 (2004).
[15] L. P. Tarasov, Phys. Rev. **56**, 1245 (1939).
[16] M. F. Collins and J. B. Forsyth, Philos. Mag. **8**, 401 (1963).
[17] H. Zabel, Appl. Phys. A: Solids Surf. **58**, 159 (1994).
[18] I. Ohnuma, H. Enokia, O. Ikeda, R. Kainuma, H. Ohtani, Bo Sundman, and K. Ishida, Acta Mater. **50**, 379 (2002).
[19] J. Ph. Jay, M. Wójcik, and P. Panissord, Z. Phys. B: Condens. Matter **101**, 471 (1996).
[20] K. Amemiya, S. Kitagawa, D. Matsumura, H. Abe, T. Ohta, and T. Yokoyama, Appl. Phys. Lett. **84**, 936 (2004).
[21] P. S. Ho, J. E. Lewis, H. S. Wildman, and J. K. Howard, Surf. Sci. **57**, 393 (1976).
[22] W. L. O'Brien and B. P. Tonner, Phys. Rev. B **50**, 2963 (1994).

[23] G. A. Prinz, Phys. Rev. Lett. **54**, 1051 (1985).
[24] D. K. G. de Boer and W. W. van den Hoogenhof, Spectrochim. Acta, Part B **46**, 1323 (1991).
[25] I. L. Soroka and B. Hjörvarsson, J. Magn. Magn. Mater. **272–276**, 1247 (2004).
[26] J. Hunter Dunn, A. Hahlin, O. Karis, D. Arvanitis, G. LeBlanc, Å Andersson, and L.-J. Lindgren, AIP Conf. Proc. No. 705 (AIP, Melville, NY, 2004), pp. 65–68.
[27] D. Weller, Y. Wu, J. Stöhr, M. G. Samant, B. D. Hermsmeier, and C. Chappert, Phys. Rev. B **49**, 12888 (1994).
[28] A. M. Blixt, G. Andersson, J. Lu, and B. Hjörvarsson, J. Phys.: Condens. Matter **15**, 625 (2003).
[29] B. T. Thole, P. Carra, F. Sette, and G. van der Laan, Phys. Rev. Lett. **68**, 1943 (1992).
[30] P. Carra, B. T. Thole, M. Altarelli, and X. Wang, Phys. Rev. Lett. **70**, 694 (1993).
[31] W. L. O'Brien and B. P. Tonner, Phys. Rev. B **50**, 12672 (1994).
[32] C. Kittel, *Introduction to Solid State Physics*, 7th ed. (Wiley, New York, 1996), p. 449.
[33] Richard M. Bozorth, *Ferromagnetism* (Van Nostrand, New York, 1956), Chap. 8.
[34] P. M. Marcus and V. L. Moruzzi, Solid State Commun. **55**, 971 (1985).
[35] See, J. S. Faulkner, Prog. Mater. Sci. **27**, 1 (1982), for a review, and A. V. Ruban, I. A. Abrikosov, and H. L. Skriver, Phys. Rev. B **51**, 12958 (1995), for the details of the KKR-CPA method.
[36] J. Stöhr, J. Magn. Magn. Mater. **200**, 470 (1999).
[37] M. Krcmar, C. L. Fu, and J. R. Morris, Mater. Res. Soc. Symp. Proc. **842**, S1.4.1 (2005).
[38] D. Bonnenberg, K. A. Hempel, and H. P. J. Wijn, in *Magnetic Properties of Metals*, edited by H. P. J. Wijn, Landolt-Börnstein, New Series, Group III, Vol. 19a (Springer-Verlag, Berlin, 1987), p. 178.